Injection and strong current channeling in organic disordered media

Tutiš, Eduard; Batistić, Ivo; Berner, Detlef

Repository / Repozitorij:

Injection and strong current channeling in organic disordered media

Eduard Tutiš*

Institute of Physics, Bijenička c. 46, P.O. Box 304, HR-10001 Zagreb, Croatia

Ivo Batistić

Department of Physics, University of Zagreb, Bijenička c. 32, P.O. Box 331, HR-10002 Zagreb, Croatia

Detlef Berner

CFG S.A. Microelectronic, CH-1110 Morges, Switzerland
(Received 27 May 2004; published 8 October 2004)

We consider charge injection from a metal into amorphous organic molecular media with correlated disorder. It is shown that correlations, known to be essential for understanding the field dependence of the carrier mobility, also strongly influence the injection current distribution. In particular, we find that the injection hot spots are intrinsic for metal/organic interfaces, even for perfectly flat surfaces. The current density variations reach several orders of magnitude for realistic material parameters. The injection hot spots further induce current channels in the bulk of the material that extend a hundred nanometers beyond the injection surface. For electronic devices based on thin amorphous organic films, as are the organic light-emitting diodes, this current channeling is expected to have a serious impact on device characteristic and performance.

PACS number(s): 73.40.Ns, 73.61.Ph

I. INTRODUCTION

The interest in electronic devices based on amorphous organic materials has been increasing during the last decade. This interest was triggered by the development of organic light-emitting devices (OLED) based on thin amorphous films of small organic molecules[1] or polymers.[2] While commercial applications based on OLED's have reached the market, the research aiming at higher efficiency and longer lifetime of these devices is intensifying. For this reason it seems that a better understanding of the processes at metal/organic and organic/organic interfaces is particularly required.

In this respect it is well known that disorder influences substantially both the bulk transport and the interface-related processes. The carrier mobility in disordered organic material has been found to be many orders of magnitude lower than in the crystalline phase. The charge transport is strongly nonlinear and the Pool-Frenkel (PF) behavior for mobility, $\log \mu \propto \sqrt{F}$, regularly found in these materials,[3] is obeyed over a wide range of electric fields. It has been found that PF behavior is essentially related[4,5] to the *spatial correlations* persisting in a disordered material. While several physical origins of correlation have been proposed, the very existence of the spatial correlation in disordered organic materials and its influence on charge transport seems to be well established.

The effect of disorder on injection has been addressed as well.[6,7] However, mostly charge injection into the material with *uncorrelated* disorder has been considered, apart from Ref. 8. The results are usually presented in terms of injection curves, which progressively differ from the Richardson-Schottky behavior as the strength of disorder increases. The physical picture behind is rather simple. The energy barrier that has to be passed by the carriers entering the organic layer is modified by disorder. Some injection paths become less favorable and some of them more favorable than in the ordered medium.

In this paper we show that the statistical distribution of favorable paths depends on the space correlation of the disorder. In particular, we consider the variation of the injection current density over the electrode surface and show that this effect is strong for realistic disorder strength. Moreover, this effect extends throughout the organic layer, thus affecting both the efficiency and lifetime of the devices based on thin organic amorphous films.

II. MODEL

The model that we start with is essentially the one that has been used for studying the injection in the system with uncorrelated disorder.[6] The only difference is that we consider correlated disorder instead. The model of correlations that we use follows the one considered by Dunlap and co-workers.[4] We start with randomly oriented electric dipoles $\vec{p}_i$ ($|\vec{p}_i| \equiv p$) occupying a regular cubic mesh with the lattice constant a. The randomly oriented dipoles produce correlated energetic disorder at molecular sites, with the correlations coming from the $1/r^2$ tail of the dipolar potential. For this type of correlated disorder Dunlap *et al.*[4] were able to derive analytically the PF mobility law in one dimension (1D) and to extend its validity to two and three dimensions (2D and 3D) by numerical simulations.[9] For 3D calculations in our paper we use the cell of $M_x \times M_y \times M_z = 64 \times 64 \times 64$ randomly oriented dipoles. The cell is then periodically repeated in space and the Coulomb energies U_i^0 are then calculated for each lattice point. The energies U_i^0 are distributed according to the distribution that is approximately Guassian[9–11] with $\langle U_i^0 \rangle = 0$ and with a width $\sigma \equiv \langle (U_i^0)^2 \rangle = 2.35qp/4\pi\varepsilon_0\varepsilon_r a^2$. Here q stands for the electron charge and $\varepsilon_0\varepsilon_r$ represents the dielectric constant of the medium.

This system is then sharply cut along the $x=0$ plane and the metal (electrode) surface is positioned there,[12] at the distance x_1 from the first monolayer of the mesh. Specifically,

we take $x_1=a/2$. A carrier of the charge q inside the organic layer experiences an image force potential due to the metal surface. The molecular energy level is then shifted to $E_i^0=U_i^0-q^2/16\pi\varepsilon_0\varepsilon_r x_i$, while the external electric field F shifts it further to $E_i=E_i^0-Fq(x_i-x_1)$.

The electron hopping is described by the master equation

$$\frac{dn_i}{dt}=\sum_\delta \nu_0[n_{i+\delta}e^{(E_{i+\delta}-E_i)/2T}-n_i e^{-(E_{i+\delta}-E_i)/2T}], \quad (1)$$

where n_i denotes the occupancy of the ith site and $i+\delta$'s are the indices of the nearest neighbors of the site i.

The injection current is calculated by imposing a steady-state solution to the master equation, while the occupancy of the leftmost and the rightmost sites is kept constant and independent of the electric field. In particular, the sites next to the metal surface are assumed to be in perfect equilibrium with the metal. Assuming also that the Fermi level of the metal μ is much below the molecular energy levels, we get

$$n_i=e^{-(E_i^0-\mu)/T} \text{ for } x_i=x_1. \quad (2)$$

The particle densities at sites at $x_i=x_1+M_x a$, next to the exiting electrode, are also fixed. Apart from very low fields these values do not influence the current values. However, by taking $n_i=\exp[-(E_i^0-\mu)/T]$ at $x_i=x_1+M_x a$ we also ensure the correct behavior at very low fields, with the limit $j(F=0)=0$ being obeyed.

III. 1D, 2D, AND 3D SOLUTIONS

For the system that is homogenous in directions perpendicular to the electric field (no disorder in the perpendicular direction or no disorder at all), the steady state may be readily found, since the current density is constant throughout the sample. Since the current in the direction perpendicular to the field vanishes, each chain of nodes in the direction of the field may be considered independently. The charge current,

$$j/j_0=n_m e^{(E_m-E_{m+1})/2T}-n_{m+1}e^{-(E_m-E_{m+1})/2T}, \quad (3)$$

is constant throughout a 1D chain. Here j_0 is defined as $j_0=q\nu_0/a^2$. Upon iterating this equation the occupancy at far site, n_m, is expressed through the occupancy of the first site in the chain, n_1,

$$n_m=n_1 e^{(E_1-E_m)/T}-(j/j_0)\sum_{l=1}^{m-1} e^{(E_l-E_{l+1})/2T+(E_l-E_m)/T}. \quad (4)$$

The condition of n_m not diverging exponentially as the distance from the electrode increases sets the value for the current,

$$j=\frac{j_0}{\sum_{m=1}^{\infty} e^{((E_m+E_{m+1})/2-\mu)/T}}. \quad (5)$$

The sum in the denominator is dominated by the term where E_m+E_{m+1} is maximal. The lower the value of this maximum, the bigger the current. In practice this sum is evaluated with minimal numerical effort since it is fast converging. In the absence of disorder, $E(x_i)=\mu+\Delta-q^2/16\pi\varepsilon_0\varepsilon_r x_i-Fqx$, where Δ stands for the difference between the molecular LUMO energy level and the Fermi level of the injecting electrode. In the low field limit the sum may be then replaced by an integral and estimated using the steepest descent method. This leads to

$$j\approx\frac{q\nu_0}{a^2}e^{-(E_{max}-\mu)/T}\sqrt{\frac{|E''_{max}|a^2}{2\pi T}}$$

$$=\frac{q\nu_0}{a^2}\left(\frac{16\varepsilon_0\varepsilon_r a^2 qF^3}{\pi T^2}\right)^{1/4}\exp\left(-\frac{\Delta}{T}+\frac{1}{T}\sqrt{\frac{Fq^3}{4\pi\varepsilon_0\varepsilon_r}}\right), \quad (6)$$

where E_{max} corresponds to the maximum of the function $E(x)$ and E''_{max} corresponds to its second derivative at the same point. The formula resembles the Richardson-Schottky thermionic injection formula, although the mechanism of the charge transport is very much different.[13]

Here we derived the formula (5) because it is not without value for considering the injection into the system with correlated disorder. Being exact for the disordered 1D system without hopping in the direction perpendicular to the field, the equation may give a good clue about injection for systems with correlated disorder in higher dimensions. This was verified through comparison with exact 2D and 3D solutions for models with transversal hopping. The reason is that correlation tends to homogenize the systems locally in the direction perpendicular to the field, thus reducing the importance of hopping in this direction. On the other hand, the 1D solution may say little about preferred current paths in the bulk of the material.

Moreover, it turns out that the procedure leading to Eq. (5) can be generalized for disordered 2D and 3D systems, thus producing an efficient numerical algorithm for calculating the injection characteristics.[14]

IV. INJECTION CURRENT DISTRIBUTION

Finding the steady state for the master equation (1) requires solving a linear system of equations with the occupancies n_i on internal nodes as the unknowns. Solving the 1D problem (with the hopping in the y and z directions being forbidden) and the 2D problem (with hopping in the y or z direction being forbidden) gives rather a good clue about the full 3D solution where hopping is present in all three directions. The 3D problem may be solved rather effectively using the appropriate sparse matrix inversion routine.[15] In order to follow the current paths into the bulk of the organic layer we consider the system of the size $64\times64\times64$, although much shorter systems (e.g., $20\times64\times64$) give already very accurate injection characteristics.[14] We use realistic parameters for the disorder in organic amorphous media.[9,3] In the example presented below the dipole strength is set to $p=3$ D (3 Debye) and the separation between nodes to $a=1$ nm, leading to the energy distribution width $\sigma\approx70$ meV. In Fig. 1 we show a typical result for the injection current distribution close to a perfect flat electrode. The electric field strength of $F=0.5$ MV/cm is taken as typical for the OLED operation (e.g., 5 V voltage drop over an organic layer which
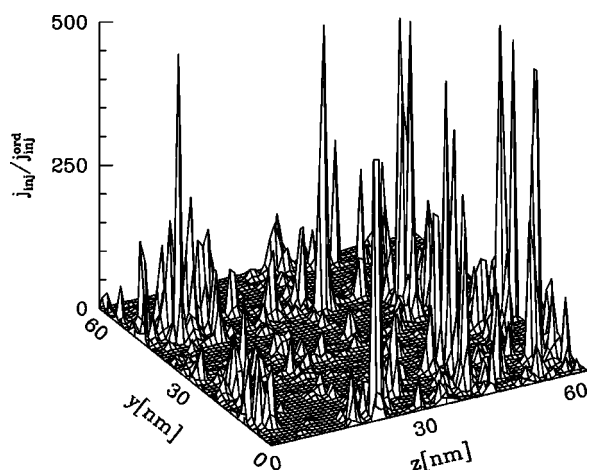
FIG. 1. The injection current distribution over the electrode surface for $F=0.5$ MV/cm and $T=300$ K. The injection current density is plotted relative to j_{inj}^{ord}, the injection current density in the absence of disorder.
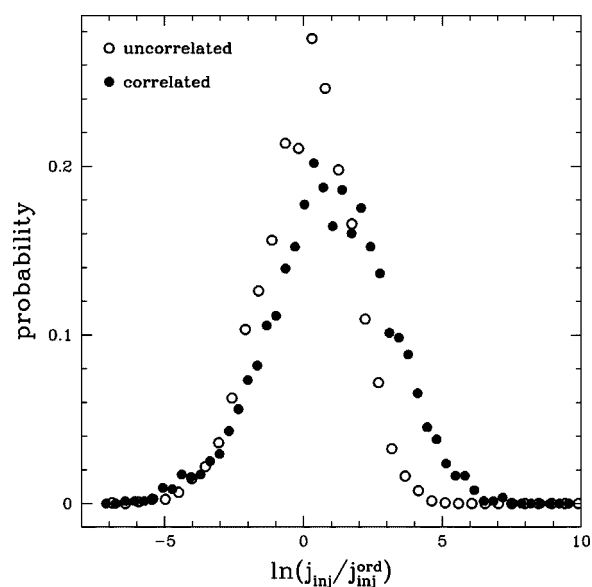

FIG. 2. The distribution of sites with respect to the value of the local injection current. The cases correspond to the correlated disorder and uncorrelated Gaussian disorder, with the same disorder strength σ. Both distributions are of the Gaussian shape when plotted against the logarithm of the current density. While the distributions do not differ at the low-current side, they do differ very much at high currents. The correlated disorder provides better injection paths. The average injected current for the correlated disorder is an order of magnitude bigger than for the uncorrelated disorder.
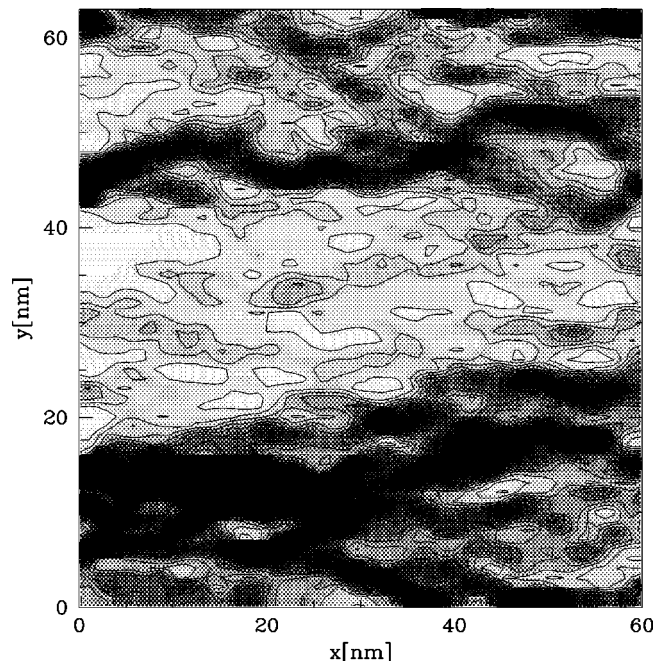
is 100 nm thick). The prominent feature of Fig. 1 is the occurrence of the regions of particularly high injection current density. These are the regions where the injecting barrier is locally lowered by disorder. These regions dominate the whole injection characteristics for a disordered medium.

It should be emphasized again that in this consideration the strong variation of the current density is not related to the roughness of the electrode.[16,17] The electrode is assumed perfectly flat and the variation is attributed solely to disorder.

The result is very much affected by the correlations in the disorder. This may be already inferred to some extent from the 1D formula in Eq. (5). It includes the factor involving *two neighboring sites*, which has to be small in order to get amplified injection. In 3D the manifold of paths is explored numerically. In order to examine the role of correlations we calculate the statistics of the current density near the metal surface for systems with and without correlations, while the disorder strength σ is kept equal. The result is presented in Fig. 2 and shows that injection inhomogeneity is indeed much more pronounced in the system with correlated disorder.

V. CURRENT CHANNELS

More important than the inhomogeneity in the close vicinity of a perfectly flat metal surface are the implications for the transport in the bulk. We find that the inhomogeneity introduced by injection persists throughout the whole organic layer of 60 nm thickness, for fields of a fraction of 1 MV/cm. The current density distribution in the direction of the applied field is illustrated in Fig. 3. These resulting current channels, formed due to correlated disorder in the electrode region, may be particularly relevant for organic electronic devices composed of organic amorphous films of thickness up to 100 nm, with the disorder strength bigger than several hundredths of electron volts and a typical driving voltage of the order of $5-10$ V.

It should be noted that current channeling is a consequence of a specific random potential configuration that is

FIG. 3. The current density distribution along the direction of the field (x direction) for $F=0.5$ MV/cm. The dark parts on this contour plot correspond to regions with high current density. The left-hand side of the figure corresponds to data in Fig. 1 for $z \approx 40$ nm. More precisely, the present figure shows the current density distribution within the slab between the planes at $z=35$ nm and $z=45$ nm. The current channels, induced by the injection hot spots near $y=10$ nm and $y=45$ nm in Fig. 1 are clearly visible.

very probable in the case of the correlated disorder. The required condition for its occurrence is a reduced potential barrier (due to the random energy level distribution) anywhere *close to the metal injection surface*. Specific random energy level distribution in the interior of the organic layer is not so important for the occurrence of current channels. Energy level distribution in the interior of the organic layer can, however, shape the pathway of the current channels. However, they are also affected by applied electric field. The *current filaments* change their shapes as the strength of applied electric field changes, always persisting through the whole organic layer.

The current channeling is not desirable in organic light-emitting diodes and related devices for at least two reasons. One is related to the device lifetime, and the other one to the device efficiency. As for the first one, it is now rather established that a high current leads to accelerated device degradation.[18] This produced rather widespread experimental practice to use high currents for accelerated OLED testing. Reduced to a microscopic level this suggests that the device will degrade faster along the channels where the current density is higher then elsewhere. As for the second one, it is desirable not to have electrons and holes taking different current channels when crossing the organic layer. Having different current paths for electrons and holes reduces the probability for exciton creation and the device efficiency. Therefore, in spite of the fact that channeling may be regarded as an intrinsic property of the hopping transport in thin disordered organic films, one may want to reduce it by any available means. In fact, the history of OLED construc-

tion is rich in various modifications, many of them related to metal/organic and organic/organic interfaces. Several of them led to device improvements, although the underlying mechanisms were not always evident.

In our simulation we tried several modifications in the region of the metal/organic interface that may lead to partial suppression of the current channeling. For example, the introduction of a 10 nm thick layer with reduced disorder next to the metal surface (so called "injection layer," proved very helpful in this respect. The introduction of a small energy barrier behind the Schottky barrier was somewhat less helpful. These and some other cases will be presented in more detail in a separate publication. However, at this point it seems to us that several device improvements that were accomplished in the past[18,19] may possibly have dealt with the reduction of the current channeling.

In conclusion, we have shown that the injection into disordered organic media is intrinsically strongly inhomogeneous. This induces current channeling in the bulk of the organic media. The spatial correlations of disorder amplify the effect very much. The mechanism of current channeling affects the performance of all organic electronic devices based on thin amorphous films. However, it may be reduced by proper modifications of the device architecture. These issues may then be effectively incorporated in elaborate full-device simulation models currently under development.[20,21]

ACKNOWLEDGMENTS

*Corresponding author. Email address: edo@ifs.hr

[1] C. W. Tang and A. Van Slyke, Appl. Phys. Lett. **51**, 913 (1987).

[2] R. H. Friend, R. W. Gymer, A. B. Holmes, J. H. Burroughes, R. N. Marks, C. Taliani, D. D. C. Bradley, D. A. Dos Santos, J. L. Brédas, M. Lögdlund, and W. R. Salaneck, Nature (London) **397**, 121 (1999) and references therein.

[3] S. Naka, H. Okada, H. Onnagawa, Y. Yamaguchi, and T. Tsutsui, Synth. Met. **111–112**, 331 (2000).

[4] D. H. Dunlap, P. E. Parris, and V. M. Kenkre, Phys. Rev. Lett. **77**, 542 (1996).

[5] Yu. N. Gartstein and E. M. Conwell, Chem. Phys. Lett. **245**, 351 (1995).

[6] Yu. N. Gartstein and E. M. Conwell, Chem. Phys. Lett. **255**, 93 (1996)

[7] U. Wolf, V. I. Arkhipov, and H. Bässler, Phys. Rev. B **59**, 7507 (1999).

[8] M. A. Baldo and S. R. Forrest, Phys. Rev. B **64**, 085201 (2001).

[9] S. V. Novikov, D. H. Dunlap, V. M. Kenkre, P. E. Parris, and A. V. Vannikov, Phys. Rev. Lett. **81**, 4472 (1998).

[10] S. V. Novikov and A. V. Vannikov, JETP **79**, 482 (1994).

[11] R. H. Young, Philos. Mag. B **72**, 435 (1995).

[12] We also considered the case when the effect of the metal surface is treated by imposing "image dipoles" behind the surface. This reduces the strength of disorder in the first two or three layers and affects the results at very high fields when the Schottky barrier comes that close to the metal surface. However, even

then, the injection inhomogeneity is much more pronounced for the system with correlated disorder and the injection current is bigger again.

[13] P. R. Emtage and J. J. O'Dwyer, Phys. Rev. Lett. **16**, 356 (1966).

[14] This also allows for a much more efficient 3D numerical method, inspired by the 1D treatment explained above. The 3D method uses an iteration procedure to obtain the charge distribution in the first sheet (monolayer) from an arbitrary current distribution at the exiting electrode. By inverting the result one then finds the current distribution throughout the system from the charge distribution in the first monolayer. Further details of this algorithm will be published separately.

[15] Apart from standards libraries, we used the SuperLU algorithm (http://crd.lbl.gov/~xiaoye/14/).

[16] D. Berner, E. Tutiš, W. Leo, M. Schaer, and L. Zuppiroli, Proc. SPIE **5464**, 330 (2004).

[17] S. V. Novikov and A. V. Vannikov, Mol. Cryst. Liq. Cryst. **384**, 55 (2002).

[18] S. A. Van Slyke, C. H. Chen, and C. W. Tang, Appl. Phys. Lett. **69**, 2160 (1996).

[19] A. B. Chwang, R. C. Kwong, and J. J. Brown, Appl. Phys. Lett. **80**, 725 (2002).

[20] E. Tutiš, M. N. Bussac, B. Masenelli, M. Carrard, and L. Zuppiroli, J. Appl. Phys. **89**, 430 (2001).

[21] H. Houili, E. Tutiš, H. Lutjens, M. N. Bussac, and L. Zuppiroli, Comput. Phys. Commun. **156**, 108 (2003).